

1
2
3
4
5
6
7
8
9
10
11
12
13
14
15
16
17
18
19
20

The origin of sub-surface source waters define the sea-air flux of methane in the Mauritanian Upwelling, NW Africa

Ian J. Brown¹, Ricardo Torres¹, Andrew P. Rees^{1*},

¹ Plymouth Marine Laboratory, Prospect Place, The Hoe, Plymouth, PL1 3DH, UK.

*** corresponding author: apre@pml.ac.uk**

21 Abstract

22 Concentrations and flux densities of methane were determined during a lagrangian study of an advective
23 filament in the permanent upwelling region off western Mauritania. Newly upwelled waters were
24 dominated by the presence of North Atlantic Central Water and surface CH₄ concentrations of 2.2 ± 0.3
25 nmol L⁻¹ were largely in equilibrium with atmospheric values, with surface saturations of $101.7 \pm 14\%$.
26 As the upwelling filament aged and was advected offshore, CH₄ enriched South Atlantic Central Water
27 from intermediate depths of 100 to 350m was entrained into the surface mixed layer of the filament
28 following intense mixing associated with the shelf break. Surface saturations increased to $198.9 \pm 15\%$
29 and flux densities increased from a mean value over the shelf of $2.0 \pm 1.1 \mu\text{mol m}^{-2}\text{d}^{-1}$ to a maximum of
30 $22.6 \mu\text{mol m}^{-2}\text{d}^{-1}$. Annual CH₄ emissions for this persistent filament were estimated at $0.77 \pm 0.64 \text{ Gg}$
31 which equates to a maximum of 0.35% of the global oceanic budget. This raises the known outgassing
32 intensity of this area and highlights the importance of advecting filaments from upwelling waters as
33 efficient vehicles for air-sea exchange.

34

35 **Keywords:** Methane, Atlantic Ocean, Upwelling, Filaments, Air-sea exchange

36

37 1. Introduction

38 Methane (CH₄) is the most abundant trace organic gas in the environment [*Wuebbles and Hayhoe, 2002*]
39 and plays an important role in the Earth's climate. It acts to limit the tropospheric oxidative capacity and
40 is radiatively active, with a global warming potential that exceeds CO₂ by 23 times over a 100 year
41 timescale [*IPCC, 2007*].

42 The world's oceans are a natural source of CH₄ but play only a minor role in its global atmospheric
43 budget [*Wuebbles and Hayhoe, 2002*], contributing up to 10% of the global atmospheric emissions
44 [*Grunwald, et al., 2009*]. That said, marine sources are not well constrained owing to a paucity of

45 observations [Forster, et al., 2009]. Coastal environments including estuaries are thought to account for
46 approximately 75% of the marine source [Bange, et al., 1994] and coastal upwelling areas have been
47 shown to be particularly rich source areas [Kock, et al., 2008; Monteiro, et al., 2006; Owens, et al., 1991].
48 Methanogenesis is an anaerobic process, which in oceanic waters is thought to occur either in oxygen
49 deplete waters or in anoxic micro-environments that are associated with zooplankton guts and particulate
50 material [Bianchi, et al., 1992; Marty et al., 1997; Brooks, et al., 1981]. In upwelling areas CH₄
51 production has been indirectly linked to the high productivity of these regions and the decomposition of
52 sinking detrital material formed therein [Rehder et al., 2002; Kock et al., 2008]. The association between
53 CH₄ production and phytoplankton biomass though is not ubiquitous. Previous studies have reported both
54 a closely coupled relationship between the two [eg. Oudot, et al., 2002, Damm et al., 2008], while others
55 have found weak or no correlation at all [Bianchi, et al., 1992; Holmes, et al., 2000].

56 The NE Atlantic upwelling of the coast of Mauritania is globally one of the most biologically productive
57 systems [Pauly and Christensen, 1995] and occurs as a consequence of off-shore Ekman transport due to
58 trade winds along the coastline [Mittelstaedt, 1991]. Despite the high productivity of this area and the
59 association of upwelling with positive fluxes to the atmosphere of methane [e.g. Owens et al., 1991, Kock
60 et al., 2008] there are relatively few studies of CH₄ in this region and those that have been performed are
61 predominately concerned with surface waters.

62 During research cruise D338 on-board RRS Discovery in April 2009 we deployed the tracer SF₆ with
63 drogued drifter buoys to track recently upwelled water and perform a lagrangian investigation [Meunier
64 et al., 2012] into CH₄ concentration and its flux with the atmosphere in an area associated with active
65 upwelling throughout the year (Fig 1).

66

67 **2. Methods**

68 A physical survey using shipboard instrumentation combined with satellite derived sea surface
69 temperature (SST) and chlorophyll-a data of the study site was performed to identify recently upwelled
70 water and the starting position for a lagrangian experiment. The aim was to track the evolution of an
71 upwelling filament using a sulfur hexafluoride (SF₆) labelled patch. SF₆ deployment was made at a depth

72 of 5m around a central buoy [Nightingale, et al., 2000] and the centre of the patch was located via on-
73 board analysis by discrete and continuous gas chromatography, the ship was repositioned daily to the
74 centre of the patch. Sea water samples were collected at 14 stations (Fig. 1) from Niskin bottles on a CTD
75 rosette with clean Tygon[®] tubing into 1L borosilicate bottles. Samples were overfilled with three times
76 the bottle volume to eliminate air bubbles and poisoned with 200µl of a saturated mercuric chloride
77 solution. They were then transferred to a water bath at 25 ± 0.1 °C and temperature equilibrated for a
78 minimum of one hour before analysis. Samples were analysed for CH₄ by single-phase equilibration gas
79 chromatography using a flame ionisation detector similar to that described by Upstill-Goddard et al.,
80 [1996].

81 Air measurements were collected from the ships fore-mast whilst on station using a diaphragm pump
82 (Charles Austen Ltd CapexL2) which was used to draw air through “Dekabon” tubing directly to the
83 ships laboratory. The gas line was purged for 5 minutes and particulates and water were removed using
84 quartz wool and magnesium perchlorate respectively prior to the introduction to the gas chromatograph.
85 Seawater samples were typically analysed within 8 hours of collection. Each individual determination of
86 dissolved and atmospheric CH₄ was calibrated against 3 certified standards 1.00, 2.04 and 3.01 ppm \pm 5%
87 (Air Products Ltd.), which were verified as such by comparison to others which are traceable to the
88 NOAA 2004 scale for CH₄ mole fractions. Instrument precision, based on measurements of the three
89 reference gases made throughout each day (n= 5 to 10 for each standard) was better than 0.77%.

90 Aqueous CH₄ concentrations were calculated from the solubility table of *Wiesenburg and Guinasso*,
91 [1979]. The CH₄ saturation in seawater was determined as the ratio of in-situ CH₄ to atmospheric samples
92 determined on board (mean 1.84 ± 0.06 ppm, compared with 1.86ppm Mace Head Ireland, 1.81 ppm
93 Ragged Point Barbados – taken from Advanced Global Atmospheric Gases Experiment (AGAGE) data
94 set – <http://agage.eas.gatech.edu> for May 2009).

95 The CH₄ exchange between the air and ocean, the sea-air flux density (F_{CH_4}) was parameterised as:

$$96 \quad F_{CH_4} = (k_w(S_c/600)^{-0.5})(C_w - C_a)$$

97 where K_w is the gas transfer coefficient [Nightingale, et al., 2000] normalised to a height of 10m [Large
98 and Pond, 1982]. C_w is the seawater concentration and C_a is the equilibrium water concentration of CH₄

99 calculated against the corresponding atmospheric measurement. S_c is the Schmidt number [Wanninkhof,
100 1992].

101 CH_4 fluxes into the surface mixed layer from deeper waters (VF_{CH_4}) were estimated from:

$$102 \quad \text{VF}_{\text{CH}_4} = K_z \times (\partial\text{CH}_4 / \partial z).$$

103 The mean gradients driving the flux into the surface layer were estimated by calculating the slope of a
104 linear fit to the available data between the deep maxima (located between 100 and 350) and the bottom of
105 the mixed layer. The values of eddy diffusivity (K_z – Fig. 2) were obtained from observations performed
106 with a free-falling shear microstructure profiler (ISW Wassermesstechnik MSS-90). Data from MSS90
107 profiles were only used at depths greater than 10m, due to the potential for contamination from the
108 motion of the ship induced by wave activity [Lozovatsky *et al.*, 2006]. Values for K_z used in the
109 calculation of VF_{CH_4} were the mean of all estimates from the closest MSS90 profiles in time and covering
110 the depth range used for calculating the methane gradient. Estimates of VF_{CH_4} should be considered as
111 conservative in part as a consequence of the low vertical sample resolution, which meant that small scale
112 gradients in methane are likely to be larger than those used here. Similarly, the broad depth range used to
113 determine eddy diffusivity is likely to provide underestimated values of K_z .

114

115 **3. Results and Discussion**

116 Upwelling off Mauritania is fed by two different subsurface water masses identified by Tomczak [1982].
117 Upwelling waters north of $\sim 20^\circ\text{N}$ are mainly influenced by North Atlantic Central Water (NACW) while
118 the area south of 20°N is dominated by South Atlantic Central Water (SACW) which is generally cooler,
119 fresher and has a higher nutrient and lower oxygen content than that of NACW [Minas, *et al.*, 1982]. The
120 percentage of each water mass present during this analysis was determined by applying optimum
121 multiparameter (OMP) analysis to temperature, salinity, nitrate and silicate profiles using the OMP
122 Package for MATLAB Version 2.0 (http://www.ldeocolumbia.edu/~jkarsten/omp_std). The upper 200m
123 of the filament were dominated by NACW (50-80%) whilst SACW dominated between 200m and 500m
124 (Fig 3). The filament was tracked for 9 days from the 21st to 29th of April 2009 over a distance of

125 approximately 200km though the filament may continue for approximately twice that distance [*Fischer,*
126 *et al.*, 2009; *Rees, et al.*, 2011]. A full description of the physical nature of this upwelling filament can be
127 found in Meunier et al., [2012] where it is referred to as Filament A. Surface waters of the 5 stations
128 occupied at the most easterly section of the filament were directly influenced by newly upwelled water,
129 which was dominated by NACW (surface temperature = $16.69 \pm 0.15^{\circ}\text{C}$) and surprisingly had the lowest
130 recorded concentrations of $2.2 \pm 0.3 \text{ nmol L}^{-1}$ (Fig. 3) and saturations ($101.7 \pm 14\%$) of CH_4 (Fig. 4). Kock
131 et al [2008] also found that surface waters associated with the NACW showed lower saturations than
132 those dominated by SACW. Although in contrast, their lowest temperatures were coincident with
133 maximum concentrations of CH_4 of 5.5 nmol L^{-1} which were associated with the upwelling of SACW
134 dominated waters at $\sim 19.5^{\circ}\text{N} \sim 17^{\circ}\text{W}$. The surface CH_4 concentration increased at the continental shelf
135 break, west of $\sim 17.6^{\circ}\text{W}$ as CH_4 enriched SACW from intermediate depths was brought to the surface.
136 The combination of enhanced turbulence (Fig 2.) at the shelf-break and strong diapycnal gradients in CH_4
137 concentration provided a strong source of CH_4 to surface waters at rates of between $170.9 \mu\text{mol m}^{-2}\text{d}^{-1}$
138 (Fig. 4) and $876.2 \mu\text{mol m}^{-2}\text{d}^{-1}$ (estimated using mean or mean +1 s.d. values of K_z respectively) Low
139 diapycnal gradients throughout the remainder of the transect resulted in VF_{CH_4} rates in the order of $1.5 \pm$
140 $1.9 \mu\text{mol m}^{-2}\text{d}^{-1}$. Surface concentrations increased to 4.2 nmol L^{-1} at 17.69°W and remained at this level
141 ($4.3 \pm 0.3 \text{ nmol L}^{-1}$, $198.9 \pm 15\%$ saturation) (Fig 3, 4) until the end of the experiment as a strong
142 westward, surface-intensified jet-like flow transported the combined NACW and SACW waters offshore
143 [Meunier et al, 2012]. Surface temperatures increased progressively to a maximum of 17.65°C at the
144 westernmost station, so that there was a strong positive correlation between temperature and CH_4
145 concentration ($r^2 = 0.69$, $n = 14$).

146 In the absence of methane oxidation rates for this study it is difficult to perform a realistic budget,
147 however we have attempted this to investigate the supply of CH_4 to the surface mixed layer for the four
148 day period between the shelf break and the end of the study. If we take our lower and upper estimates for
149 VF_{CH_4} of $170.9 \mu\text{mol m}^{-2}\text{d}^{-1}$ and $876.2 \mu\text{mol m}^{-2}\text{d}^{-1}$ and maintain a 50m mixed layer integrated CH_4
150 concentration of $215 \mu\text{mol m}^{-2}$ and losses to the atmosphere of $70 \mu\text{mol m}^{-2}$ it becomes apparent that the

151 lower estimate of VF_{CH_4} is insufficient to maintain the water column concentrations observed. To
152 provide a balanced budget the higher estimate of VF_{CH_4} would require consumption of CH_4 in the order
153 of $600 \mu\text{mol m}^{-2} 4\text{d}^{-1}$, which equates to a quite realistic rate of $\sim 3 \text{ nmol L}^{-1} \text{ d}^{-1}$, see for example Mau et
154 al., [2013]. Whilst recognising the limitations of this exercise it would allow some confidence that the
155 vertical flux of CH_4 from intermediate depths to the surface mixed layer is at the higher end of our
156 estimated range.

157 The relationship between CH_4 production and phytoplankton biomass or productivity is inconsistent. A
158 number of authors report a positive correlation between chlorophyll-a and CH_4 , for example Damm et al.,
159 [2008], who described a strong association between a summertime phytoplankton bloom and
160 methanogenesis. CH_4 production in other upwelling areas has been linked indirectly to enhanced
161 productivity through the microbial degradation of sinking material at intermediate depths below the
162 mixed layer [e.g. Rehder et al., 2002]. During the current study CH_4 showed a weak inverse relationship
163 ($r^2 = 0.43$, $n = 7$) with chlorophyll-a as can be inferred from Fig. 4. Further to this, there was no observed
164 difference between surface samples taken either at local noon or those collected before dawn (4.3 ± 0.28
165 nmol L^{-1} , $198.3 \pm 12.9\%$ compared with $4.3 \pm 0.55 \text{ nmol L}^{-1}$, $200.2 \pm 26.9\%$ for mid-day and pre-dawn at
166 off-shelf stations; and $2.6 \pm 0.33 \text{ nmol L}^{-1}$, 118.7 ± 14.1 compared with $2.1 \pm 0.2 \text{ nmol L}^{-1}$, $94.9 \pm 8.9\%$ for
167 mid-day and pre-dawn on- shelf stations). The lack of a diurnal signal in CH_4 concentration and the
168 inverse relationship between CH_4 and chlorophyll-a suggests that CH_4 supply is largely independent of
169 photosynthesis and zooplankton activity. This supports our contention that the elevated surface
170 concentrations are derived from intermediate waters (maximum concentration of 7.7 nmol L^{-1} and
171 322.4% saturation occurring at a depth of 300m) dominated by SACW rather than from in-situ
172 production (Fig. 3).

173 These surface data are in agreement with those previously published for this area ($\sim 2 \text{ nmol L}^{-1}$ – Rhee
174 2000; $2.1 - 5.5 \text{ nmol L}^{-1}$ - Kock et al., 2008; $3 \pm 0.7 \text{ nmol L}^{-1}$ - Forster et al., 2009;). Kock et al argue
175 that some of the variability between datasets may be associated with seasonal and inter-annual variability.
176 It is evident from our study that the dynamic nature of this environment and the contrasting CH_4 signature

177 between NACW and SACW lead to extremely heterogeneous vertical and horizontal distributions.
178 Geographical location with respect to upwelling waters can contribute as much to the variability
179 described as seasonal differences.

180 Eastern boundary upwelling regions are dominated by consistent winds which drive offshore water
181 movement via filaments.. The average wind speed during the current study was 10.7ms^{-1} (Fig. 4) and was
182 consistently from the north north-east which proved to be sufficient to maintain upwelling [Meunier et
183 al., 2012] and a positive sea to air flux of CH_4 for the duration of the filament. F_{CH_4} was determined using
184 wind speed determined at the time of water collection (Fig 4). The dependence of K_{W} and thus F_{CH_4} on
185 wind speed becomes obvious in Fig. 4 where daily changes in wind speed at 3 stations between 17.69°W
186 and 17.84°W of 9.5 , 15.1 and 7.2ms^{-1} result in flux densities of 14.4 , 20.3 and $10.2\text{ }\mu\text{mol m}^{-2}\text{d}^{-1}$ for
187 concentrations of 4.2 , 3.9 and 4.1 nmol L^{-1} respectively. As surface CH_4 concentrations increased with
188 progression of the filament away from the shelf-break, flux densities were found to increase by almost 8
189 times from $2.0 \pm 1.1\text{ }\mu\text{mol m}^{-2}\text{d}^{-1}$ for the first 7 stations located over the continental shelf to 17.7 ± 4.4
190 $\mu\text{mol m}^{-2}\text{d}^{-1}$ for the remaining 7 stations. The on-shelf flux densities are similar to those previously
191 reported ($2.31 - 4.04\text{ }\mu\text{mol m}^{-2}\text{d}^{-1}$ – Forster et al., 2009; $0.4 - 1.7\text{ }\mu\text{mol m}^{-2}\text{d}^{-1}$ – Kock et al., 2008), whilst
192 those determined off the shelf and influenced by upwelling of SACW influenced waters are between 5.6
193 and 13.3 times those estimated by Forster and Kock respectively. It should be noted in any comparison,
194 that each of these studies occupied geographically distinct areas and were at different times of the year.
195 The current study was in the area of permanent upwelling [Mittelstaedt, 1991] north of 20°N in April,
196 Forsters study (4 stations) transected the area in September , and the study of Kock was performed during
197 February and March, largely associated with the area of seasonal upwelling [Wooster, et al., 1976] south
198 of 20°N .

199 The heterogeneous nature of this region with respect to CH_4 concentration and flux densities coupled
200 with the highly complex oceanography and the inherent transience of these advecting filaments make it
201 difficult to extrapolate over large scales. The lagrangian approach to this study however gives us
202 confidence in our ability to characterise the nature of sea to air flux associated with this filament. Given

203 that the position of the filament was north of 20°N we consider it to be in an area of persistent upwelling
204 which allows the extrapolation of flux densities determined here over a 12 month period. In a similar
205 approach to that taken by Kock et al [2008] we have taken our mean flux density over the whole filament
206 of $10.17 \pm 8.51 \mu\text{mol m}^{-2}\text{d}^{-1}$ and using our estimate for the mean area of the filament of $1.29 \times 10^4 \text{ km}^2$
207 [Rees et al., 2011] propose an annual CH_4 emission of $0.77 \pm 0.64 \text{ Gg}$. This compares to emissions
208 estimated by Kock et al of 1.6 to 2.9 Gg y^{-1} , for an area 20 times larger than the filament examined here,
209 and contributes up to 0.35% of global estimates provided by Bates et al., [1996] for an area equivalent to
210 0.009% of the global surface ocean.

211

212 **5. Conclusion**

213 Upwelling waters close to the Mauritanian coast in the persistent upwelling found to the north of 20°N
214 are dominated by NACW which has a relatively low CH_4 signal of $2.2 \pm 0.3 \text{ nmol L}^{-1}$ which is
215 comparable to offshore waters west of 20°W [Rhee et al., 2009]. As upwelling filaments are advected
216 offshore CH_4 enriched SACW is entrained into the surface mixed layer following turbulent mixing
217 associated with the shelf break. The general uniformity of the prevailing trade winds combined with the
218 resultant high concentrations of surface CH_4 , similar to those observed in upwelling SACW south of
219 20°N, provide a strong source of CH_4 to the atmosphere. Short-term variability in the magnitude of the
220 prevailing wind fields highlighted the sensitivity of density flux estimates to wind speed. The relatively
221 small area represented by this permanently upwelling region provides a hot-spot of CH_4 emissions
222 relative to non-upwelling waters of the adjacent North Atlantic and these data emphasise the need to
223 comprehensively account for the contribution of advecting upwelling filaments to global budgets.

224

225 **6. Acknowledgements**

226 We would like to thank Carol Robinson Chief Scientist of D338, The SF6 team, Jenny Andrews for data
227 management, Claire Widdicombe for chlorophyll data, Lisa Al-Moosawi for GC development, Beatriz

228 Barreiro for water mass calculations, Ben Taylor & NEODAAS. This work was supported by NERC
229 grant NE/C517176/1 and further NERC funding to the Plymouth Marine Laboratory.

230

231 **Figure Legends**

232 **Figure 1:** MODIS – Aqua chlorophyll-a image of the Mauritanian upwelling. Station positions
233 occupied between the 21 and 29 April 2009 are identified by black squares and direction of transit
234 indicated by the black arrow. *Images courtesy of NEODAAS.*

235

236 **Figure 2:** Eddy diffusivity (K_z) determined from observations performed with a free-falling shear
237 microstructure profiler (ISW Wassermesstechnik MSS-90) within an advecting filament in the
238 Mauritanian upwelling during April 2009. The solid symbols and line represent the mean value from
239 repeated profiles, whilst the dashed line indicates the positive standard deviation of this estimate.
240 Standard deviation is not shown east of 17.5 west due to the highly turbulent nature of the on-shelf
241 upwelling waters..

242

243 **Figure 3:** Contour profiles of CH_4 concentration (nmol L^{-1}) during a lagrangian study of an
244 advecting filament in the Mauritanian upwelling during April 2009. Contoured isolines are for
245 temperature ($^{\circ}\text{C}$), data points indicated by \bullet . The dashed line indicates the approximate position of the
246 50:50 boundary between NACW and SACW. *Image produced using Ocean Data View*
247 (<http://odv.awi.de/>).

248

249 **Figure 4:** The flux of CH_4 during a lagrangian study of an advecting filament in the Mauritanian
250 upwelling relative to daily measurements of wind speed at 10m in the top panel, chlorophyll-a (bold line)
251 and sea surface temperature (dotted line) in the middle panel. In the bottom panel F_{CH_4} is shown as grey
252 bars, VF_{CH_4} as the bold line and CH_4 saturation indicated by the dashed line. The shaded area represents
253 the bathymetric profile.

254

255

256 **References**

257 Bange, H. W., et al. (1994), Methane in the Baltic and North Seas and a Reassessment of the Marine
258 Emissions of Methane, *Global Biogeochem. Cycles*, 8, 465-480.

259
260 Bates, T.S., et al. (1996), A reevaluation of the open ocean source of methane to the atmosphere, *J.*
261 *Geophys. Res.-Atmos.*, 101 6953-6961.

262
263 Bianchi, M., et al. (1992), Strictly Aerobic and Anaerobic-Bacteria Associated with Sinking Particulate
264 Matter and Zooplankton Fecal Pellets, *Mar. Ecol. Prog. Ser.*, 88, 55-60.

265
266 Brooks, J. M., et al. (1981), Methane in the Upper Water Column of the Northwestern Gulf-of-Mexico, *J.*
267 *Geophys. Res. -Oceans and Atmos.* , 86, 1029-1040.

268
269 Damm, E., et al. (2008). Methane cycling in Arctic shelf water and its relationship with phytoplankton
270 biomass and DMSP. *Mar Chem* 109, 45-59

271
272 Fischer, G., et al. (2009), Offshore advection of particles within the Cape Blanc filament, Mauritania:
273 esults from observational and modelling studies, *Prog. Oceanogr.*, 83, 322–330,
274 doi:10.1016/j.pocean.2009.07.023.

275
276 Forster, G., et al. (2009), Nitrous oxide and methane in the Atlantic Ocean between 50 degrees N and 52
277 degrees S: Latitudinal distribution and sea-to-air flux, *Deep-Sea Res. II-Topical Studies in*
278 *Oceanography*, 56, 964-976.

279
280 Grunwald, M., et al. (2009), Methane in the southern North Sea: Sources, spatial distribution and
281 budgets, *Est. Coast. Shelf Sci.* , 81, 445-456.

282
283 Holmes, M. E., et al. (2000), Methane production, consumption, and air-sea exchange in the open ocean:
284 An evaluation based on carbon isotopic ratios, *Global Biogeochem. Cycles*, 14, 1-10.

285
286 IPCC: Climate Change 2007: The Physical Science Basis, Contribution of Working Group I to the Fourth
287 Assessment Report of the Intergovernmental Panel on Climate Change, Cambridge University Press,
288 Cambridge, UK and New York, NY, USA, 996 pp., 2007.

289

290 Kock, A., et al. (2008), Methane emissions from the upwelling area off Mauritania (NW Africa),
291 *Biogeosciences*, 5, 1119 - 1125.
292

293 Large, W. G., and S. Pond (1982), Sensible and Latent-Heat Flux Measurements over the Ocean, *J. Phys.*
294 *Oceanogr.*, 12, 464-482.
295

296 Lozovatsky, I., et al. (2006), Sheared turbulence in a weakly stratified upper ocean. *Deep-Sea Res. I*: 53,
297 387-407.
298

299 Marty, D., et al. (1997), Methanoarchaea associated with sinking particles and zooplankton collected in
300 the Northeastern tropical Atlantic, *Oceanologica Acta*, 20, 863-869.
301

302 Mau, S., et al (2013), Vertical distribution of methane oxidation and methanotrophic response to elevated
303 methane concentrations in stratified waters of the Arctic fjord Storfjorden (Svalbard, Norway).
304 *Biogeosci.*, 10, 6267–6278.
305

306 Meunier, T., et al (2012), Upwelling filaments off Cap Blanc: Interaction of the NW African upwelling
307 current and the Cape Verde frontal zone eddy field?, *J. Geophys. Res.*, 117, C08031,
308 doi:10.1029/2012JC007905
309

310 Minas, H. J., et al. (1982), An Analysis of the Production-Regeneration System in the Coastal Upwelling
311 Area Off Nw Africa Based on Oxygen, Nitrate and Ammonium Distributions, *J. Mar. Res.*, 40, 615-641.
312

313 Mittelstaedt, E. (1991), The Ocean Boundary Along the Northwest African Coast - Circulation and
314 Oceanographic Properties at the Sea-Surface, *Progr. Oceanogr.*, 26, 307-355.
315

316 Monteiro, P. M. S., et al. (2006), Variability of natural hypoxia and methane in a coastal upwelling
317 system: Oceanic physics or shelf biology?, *Geophys. Res. Lett.*, 33, L16614.
318

319 Nightingale, P. D., et al. (2000), In situ evaluation of air-sea gas exchange parameterizations using novel
320 conservative and volatile tracers, *Glob. Biogeochem. Cycle*, 14, 373-387.
321

322 Oudot, C., et al. (2002), Transatlantic equatorial distribution of nitrous oxide and methane, *Deep-Sea Res.*
323 *I*, 49, 1175-1193.
324

325 Owens, N. J. P., et al. (1991), Methane flux to the atmosphere from the Arabian Sea, *Nature*, 354, 293-
326 296.

327

328 Pauly, D., and V. Christensen (1995), Primary Production Required to Sustain Global Fisheries, *Nature*,
329 374, 255-257.

330

331 Rees, A. P., et al. (2011), The Lagrangian progression of nitrous oxide within filaments formed in the
332 Mauritanian upwelling, *Geophys. Res. Lett.*, 38, L21606.

333

334 Rehder, G., et al (2002) Enhanced marine CH₄ emissions to the atmosphere off Oregon caused by coastal
335 upwelling, *Glob. Biogeochem. Cycles*, 16, 1081, doi:10.1029/2000GB001391, 2002.

336

337 Rhee, T. S., et al. (2009), Methane and nitrous oxide emissions from the ocean: A reassessment using
338 basin-wide observations in the Atlantic, *J. Geophys. Res. - Atmos.*, 114, D12304,
339 doi:10.1029/2008JD011662.

340

341 Schubert, C. J., et al. (2011), Evidence for anaerobic oxidation of methane in sediments of a freshwater
342 system (Lago di Cadagno), *Fems Microbiol. Ecol.*, 76, 26-38.

343

344 Tomczak, M. (1982), The distribution of water masses at the surface as derived from T-S diagram
345 analysis in the CINECA area, *Rapp. P. V. Reun. Cons. Int. Explor. Mer*, 180, 48–49.

346

347 UpstillGoddard, R. C., et al. (1996), Simultaneous high-precision measurements of methane and nitrous
348 oxide in water and seawater by single phase equilibration gas chromatography, *Deep-Sea Res. I*, 43,
349 1669-1682.

350

351 Wanninkhof, R. (1992), Relationship between Wind-Speed and Gas-Exchange over the Ocean, *J.*
352 *Geophys. Res.-Oceans*, 97, 7373-7382.

353

354 Wiesenburg, D. A., and N. L. Guinasso (1979), Equilibrium Solubilities of Methane, Carbon-Monoxide,
355 and Hydrogen in Water and Sea-Water, *J. Chem. Engin. Data*, 24, 356-360.

356

357 Wooster, W. S., et al. (1976), Seasonal Upwelling Cycle Along Eastern Boundary of North-Atlantic, *J.*
358 *Mar. Res.*, 34, 131-141.

359

360 Wuebbles, D. J., and K. Hayhoe (2002), Atmospheric methane and global change, *Earth-Sci. Rev.*, 57,
361 177-210.
362

363

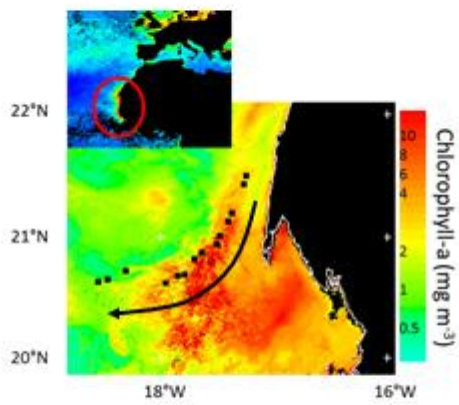


Fig 1

364

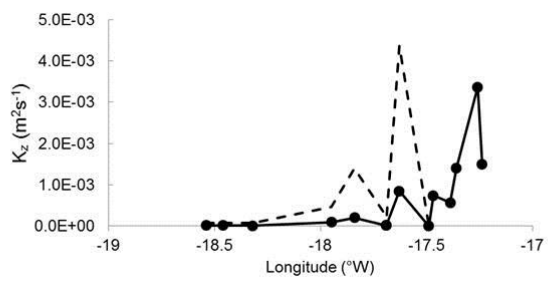


Fig 2

365

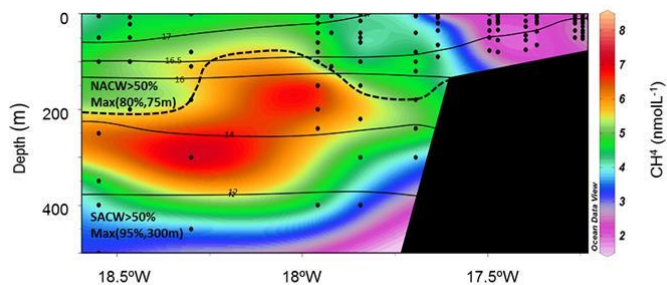


Fig 3

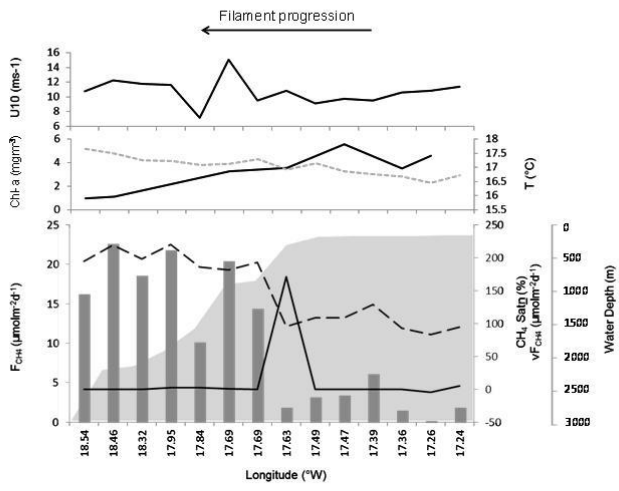


Fig 4